PROCEEDINGS OF SPIE

SPIEDigitalLibrary.org/conference-proceedings-of-spie

Assembly of a PDT device with a near-infrared fluorescence monitoring of PpIX during treatment

Marlon R. Garcia, Sebastião Pratavieira, Lilian T. Moriyama, Cristina Kurachi, Daniel V. Magalhães

Marlon R. Garcia, Sebastião Pratavieira, Lilian T. Moriyama, Cristina Kurachi, Daniel V. Magalhães, "Assembly of a PDT device with a near-infrared fluorescence monitoring of PpIX during treatment," Proc. SPIE 10860, Optical Methods for Tumor Treatment and Detection: Mechanisms and Techniques in Photodynamic Therapy XXVIII, 108600T (28 February 2019); doi: 10.1117/12.2507344

SPIE.

Event: SPIE BiOS, 2019, San Francisco, California, United States

Downloaded From: https://www.spiedigitallibrary.org/conference-proceedings-of-spie on 11 Mar 2019 Terms of Use: https://www.spiedigitallibrary.org/terms-of-use

Assembly of a PDT device with a near-infrared fluorescence monitoring of PpIX during treatment

Marlon R. Garcia[a], Sebastião Pratavieira[b], Lilian T. Moriyama[b], Cristina Kurachi[b], and Daniel V. Magalhães[a]

[a]Dept. of Mechanical Engineering, University of São Paulo, 400 Trabalhador São-carlense Av., São Carlos, Brazil

[b]São Carlos Institute of Physics, University of São Paulo, 400 Trabalhador São-carlense Av., São Carlos, Brazil

ABSTRACT

This paper describes the assembly and characterization of a system to treat and monitor ALA-based photodynamic therapy, using near-infrared fluorescence images for photosensitizer monitoring. The system is portable, user friendly and low cost, using a diode laser emitting at 633 nm as treatment light, capable to delivery up to 150 mW/cm^2 at the lesion surface. The PpIX fluorescence is excited by the treatment light itself, and detected by camera in real-time. Since the excitation and emission wavelengths are in the red-NIR spectral regions, the penetration into the skin is improved and the volume measured by the fluorescence images is larger when compared to the widely used violet excitation.

Keywords: Photodynamic therapy monitoring, dosimetry, PpIX NIR fluorescence, real-time

1. INTRODUCTION

Photodynamic therapy (PDT) has been applied for the treatment of several types of cancer lesions along the last decades.[1–3] One type of lesions for which PDT has achieved satisfatory outcomes and important development is the non-melanoma skin cancer.[4–8] One of the most prominent photodynamic procedures to treat this type of lesion is the one based on the application of δ-aminolevulinic acid (ALA), or some of its derivatives (like methyl aminolevulinate, MAL).[4–8] These substances are the precursors of protoporphyrin-IX (PpIX), the photosensitizer (PS) that can interact with light irradiation and molecular oxygen in order to generate singlet oxygen ($^1O_2$) and other cytotoxic species inducing the cell death of tumoral tissue.[9,10]

Although the important advances in the photodynamic treatment of non-melanoma skin lesions, PDT has not been chosen by the great majority of physicians around the medical field. This lack of adoption could be at least partially explained by the high variation in the treatment outcomes for different patients and different lesions, in addition to unpredicted partial responses or non-responses that an unmonitored treatment can lead.[11] Since the PDT reaction monitoring could provide a prediction of the treatment outcome, this approach becomes highly recommended towards a more individualized and optimized irradiation planing for photodynamic therapy.[11]

One technique that has been promising as a PDT dosimetric technique is the measurement of PS fluorescence.[11,12] The measurement of this quantity could give us the PS relative amount in the lesion and, as a function of time, the relative photobleaching, an indicator of cell death and treatment efficacy.[13–15] When this technique is applied, the usually chosen option is the point probe measurement, exciting the PS in the Soret band (region with the highest light absorption, Figure 1), around 405 nm, and collecting the fluorescence response from 620 nm to 720 nm.[11,13,16–18] Point probe measurements, however, could vary greatly throughout the lesion, and cannot give a profile information of PS concentration into the tissue. In case when widefield fluorescence technique is adopted, the usual excitation wavelength is also around 405 nm region, reaching the high absorption peak of Soret band, and generating a strong fluorescence around 633 nm.[12,14,19–21]

Further author information: (Send correspondence to C.K., S.P. or M.R.G.)
C.K.: E-mail: cristina@ifsc.usp.br
S.P.: E-mail: prata@ifsc.usp.br
M.R.G.: E-mail: marlonrg@gmail.com

Optical Methods for Tumor Treatment and Detection: Mechanisms and Techniques in Photodynamic Therapy XXVIII, edited by David H. Kessel, Tayyaba Hasan, Proc. of SPIE Vol. 10860, 108600T
© 2019 SPIE · CCC code: 1605-7422/19/$18 · doi: 10.1117/12.2507344

Downloaded From: https://www.spiedigitallibrary.org/conference-proceedings-of-spie on 11 Mar 2019
Terms of Use: https://www.spiedigitallibrary.org/terms-of-use

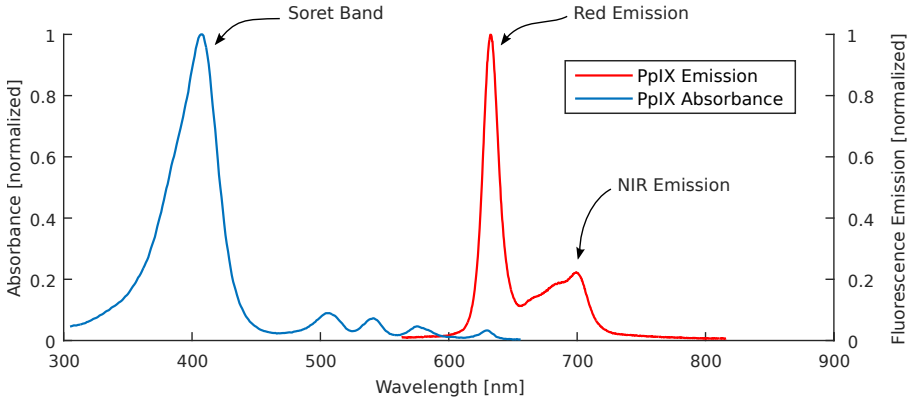

Figure 1. Absorbance spectrum of protoporphyrin-IX dissolved in dimethyl sulfoxide (DMSO) and its fluorescence emission for an excitation around 405 nm.

In order to avoid the shallow penetration of violet range into the skin, due to the strong absorption peaks and the high scattering coefficients for skin constituents at this wavelength, it is convenient to excite PpIX around 633 nm, and collect its fluorescence around 700 nm, in the NIR region. Some authors have reported the use of the red-excited PpIX fluorescence around 700 nm for PDT image monitoring.[22–24] In these cases, the described instrumentation was not capable to monitor PDT in real-time during the light dose delivery, and does not provide a treatment light with the normally chosen values of irradiance for PDT protocols (up to 125 mW/cm^2).

In the present paper we describe the development of a PDT device capable to deliver the irradiation with a controlled irradiance up to 150 mW/cm^2 at the lesion surface, and with a real-time monitoring (or dosimetry) via fluorescence images at the NIR region (around 700 nm). The monitored fluorescence is excited with the treatment light itself, around 633 nm, enabling a real-time dosimetry, even during the light dose delivery.

2. MATERIALS AND METHODS

2.1 Developed prototype

The developed prototype can be divided into three main parts: the emission, the detection and the electronic parts. All the three parts were built into a portable case (8 cm × 33 cm × 37 cm) and a 3D printed handle probe (7 cm × 12 cm × 10 cm). Together with the electronic part, a Labview (National Instruments, EUA) program was developed to control the equipment through a laptop computer.

The emission part comprises a laser module, emitting at 633 nm, an optical fiber and the emission filter. The laser module was cooled by a Peltier cell, and its emission light was coupled into a medical fiber with a 600 μm core. The emission filter, placed inside the handle probe, was used to avoid wavelengths around 700 nm (the signal to be detected) from reaching the lesion surface.

The detection part comprises a digital camera, an emission filter and a photodetector, all placed inside the handle probe, together with an acquisition board USB 6008 (National Instruments) positioned into the case. The photodetector was used to monitor the light irradiance from the optical fiber, and the emitting filter to select the fluorescence signal from PpIX, around 700 nm.

2.2 Sensor linearity and sensitivity

For the measurement of sensor linearity and sensitivity in the detection of protoporphyrin-IX, liquid phantoms were prepared in order to simulate the human skin tissue. The phantom was composed by 99 % of deionized water and 1 % of Lipofundin MCT/LCT 20 % (B.Braun Melsungen AG, Germany). Being a lipid emulsion with predominantly scattering elements, the phantom simulate the scattering properties of human skin. To simulate a skin lesion that extends from the skin surface to deeper regions of the tissue, a small tube of glass (less than 4 mm in diameter) with a PpIX solution was placed into the liquid phantom, as schematically shown in Figure 2,

Downloaded From: https://www.spiedigitallibrary.org/conference-proceedings-of-spie on 11 Mar 2019
Terms of Use: https://www.spiedigitallibrary.org/terms-of-use

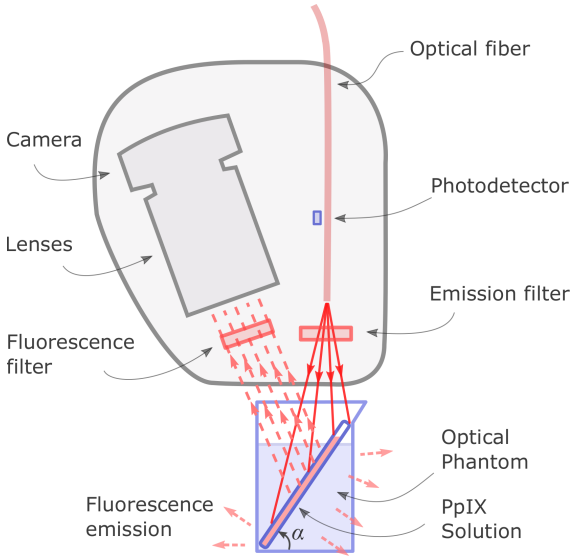

Figure 2. Schematic draw of the handle probe measuring the PpIX solution tube inside the liquid phantom for the linearity and sensitivity experiment.

placed at an angle α of 46 degrees. The PpIX solutions were all prepared in DMSO (Dimethyl sulfoxide), with concentrations ranging from 50 nM to 20 μM.

By capturing fluorescence images with the camera for all PpIX solutions prepared, it was possible to acquire the fluorescence intensity related to each PpIX concentration. The images were not pre-processed and the fluorescence intensities were acquired from the pixel intensities. For each measurement, the pixel intensity chosen as the fluorescence intensity was in the middle of the glass tube containing PpIX, in the region where the tube gets immersed into the phantom. In all the measurements, it was attempted to maintain the phantom position in relation to the measuring system, changing just the glass tub with the PpIX solution.

2.3 Phantom experiment

To test the developed equipment, a tissue-like phantom was prepared. Containing 2 % of Lipofundin MCT/LCT 20 % (B.Braun Melsungen AG, Germany) and 1.7×10^{-4} % of Nankin (Trident, Brazil), the phantom mimicked the optical properties of a skin tissue. With an agar bases, the phantom was prepared with 5 % by mass of Agar (A7002, from Sigma-Aldrich, EUA), and a PpIX concentration of 20 μM. The experimental setup was similar to that shown in Figure 2, but with the prepared agar phantom in place of the becker with the previous liquid phantom.

The equipment was used to apply a treatment-like light irradiation, with an irradiance of approximately 115 mW/cm^2, acquiring images every 30 seconds. To monitor the fluorescence intensity, a ROI (region of interest) was chosen in the fluorescence images, in the meddle of the optical spot applied. The pixel intensities inside the ROI was evaluated, and the mean of the intensities was considered as the fluorescence intensity. This experiment was conducted for about 10 hours, and all the fluorescence intensities acquired were divided by the irradiance value measured by the system's photodetector for value correction.

3. RESULTS

3.1 Sensor linearity and sensitivity

By proceeding as described above, it was possible to acquire the fluorescence intensity for each concentration studied, as shown in Figure 3 (in a log-log scale) represented by blue stars. The red dashed line in this figure represents the fitting curve, and was calculated as a first degree equation to fit the data from the four higher concentrations (1 μM, 5 μM, 10 μM and 20 μM). Although it is straight line, it appears curved in a log-log scale because does not cross the fluorescence axis in the origin.

Downloaded From: https://www.spiedigitallibrary.org/conference-proceedings-of-spie on 11 Mar 2019
Terms of Use: https://www.spiedigitallibrary.org/terms-of-use

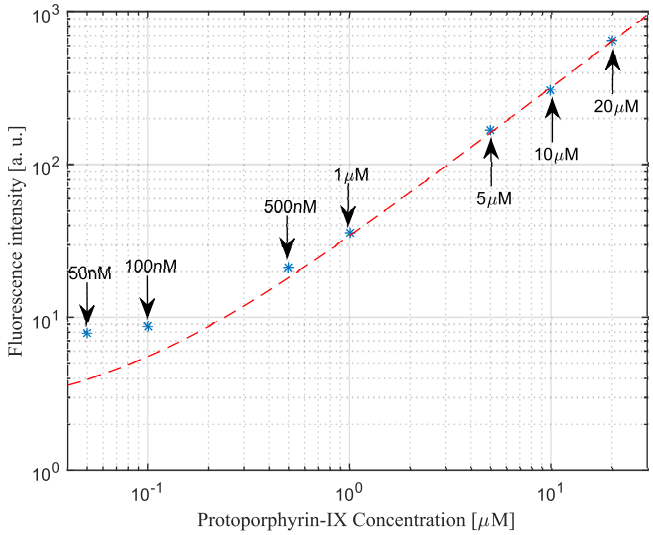

Figure 3. Fluorescence intensity per protoporphyrin-IX concentration in the experiment of linearity and sensitivity, and the fitting curve (red, dashed line) calculated to fit the concentrations from 1μM to 20μM by the method of least squares.

3.2 Phantom experiments

The phantom experiment used to simulate a PDT application and monitoring produce the fluorescence intensities shown in Figure 4, presented normalized as a function of the light dose. In the Figure 5 are presented some of the fluorescence images acquired in the experiment, for different values of light dose delivery, in false colors.

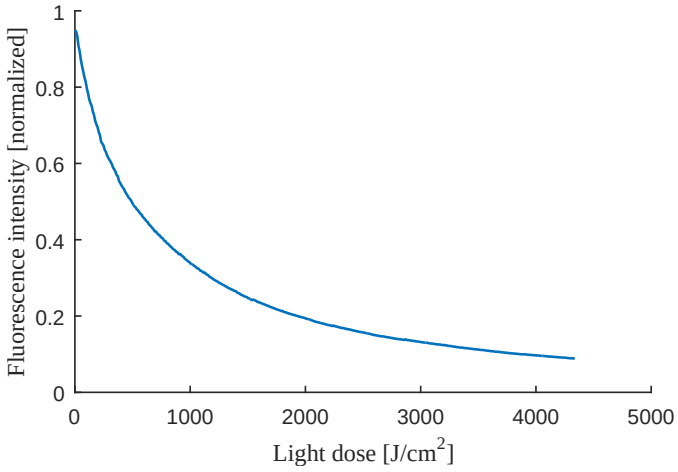

Figure 4. Fluorescence intensity normalized, as a function of the light dose applied, for the images acquired in the phantom experiment.

4. DISCUSSION

Despite the low absorbance around 633 nm (about 30 times smaller than in Soret band) and the small fluorescence around 700 nm (about 5 times smaller than in 633 nm), it was possible to monitor the red-excited PpIX fluorescence around 700 nm during the treatment light irradiation. Even providing a NIR fluorescence, which requires a camera to be detected, and producing a light signal several times smaller than the violet-excited one, the red-excited fluorescence can monitor a larger volume of tissue, due to the improved penetration in the

Downloaded From: https://www.spiedigitallibrary.org/conference-proceedings-of-spie on 11 Mar 2019
Terms of Use: https://www.spiedigitallibrary.org/terms-of-use

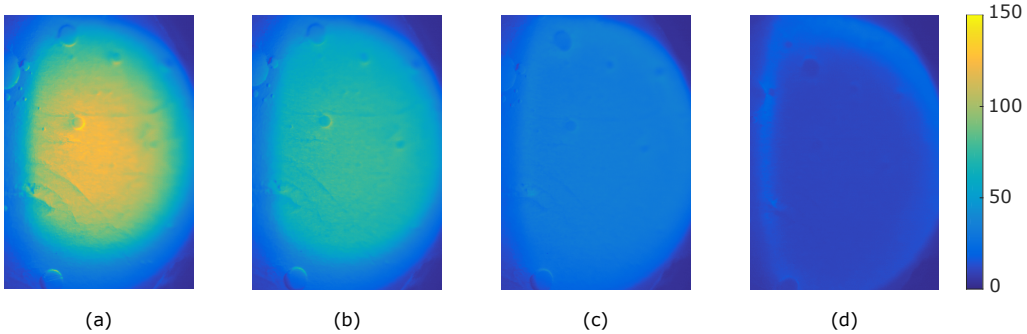

Figure 5. Fluorescence images acquired with the system, for 0 J/cm^2 (a), 350 J/cm^2 (b), 1400 J/cm^2 (c) and 4470 J/cm^2 of PDT dose delivered, in false colors. The detection wavelength centered at 700 nm, and the excitation was around 633 nm with an irradiance of about 115 mW/cm^2.

red-infrared spectral range. Moreover, this fluorescence is also excited by the treatment light itself, which allows a real-time monitoring during the treatment, without the interruption of light delivery.

The sensor linearity and sensitivity obtained were similar to thouse found in the literature for the red-excited fluorescence around 700 nm,[25] and the solution with 500 nM of PpIX could be clearly detected in the fluorescence images. The exponential fluorescence decay observed (Figure 4) was similar to the ones described in the literature, but with a slower decay curve due to, probably, the small oxygen concentration and diffusion inside the solid phantom. This slower decay is very similar to the case where PDT is applied with low oxygen concentrations.

5. CONCLUSIONS

Being an user friendly, low cost, portable system, the developed device is suitable to be used in clinical trials, and could afford a convenient translation into a commercial platform. The adoption of PDT monitoring systems would be an important step towards a customized clinical protocol, which could provide a treatment dedicated to each specific lesion in each specific person. This protocol flexibility would adapt its therapeutics parameters in order to improve the outcomes, based on a monitoring system that could aid in predicting the lesion responses. Ultimately, the more optimized use of PDT could increase its advantages over the other methods, broadening adoption around the medical field for non-melanoma skin cancer.

ACKNOWLEDGMENTS

The authors acknowledge the support provided by Brazilian Funding Agencies: Coordenação de Aperfeiçoamento de Pessoal de Nível Superior - Brasil (CAPES) - Finance Code 001; CNPq and São Paulo Research Foundation (FAPESP) grants: 2013/07276-1 (CEPOF); 2014/50857-8 (INCT).

REFERENCES

[1] Agostinis, P., Berg, K., Cengel, K. A., Foster, T. H., Girotti, A. W., Gollnick, S. O., Hahn, S. M., Hamblin, M. R., Juzeniene, A., Kessel, D., et al., "Photodynamic therapy of cancer: an update," *CA: a cancer journal for clinicians* **61**(4), 250–281 (2011).

[2] Brown, S. B., Brown, E. A., and Walker, I., "The present and future role of photodynamic therapy in cancer treatment," *The lancet oncology* **5**(8), 497–508 (2004).

[3] Henderson, B. W. and Dougherty, T. J., "How does photodynamic therapy work?," *Photochemistry and photobiology* **55**(1), 145–157 (1992).

[4] Bagnato, V., Kurachi, C., Ferreira, J., Marcassa, L., Sibata, C., and Allison, R., "Pdt experience in brazil: a regional profile," *Photodiagnosis and photodynamic therapy* **2**(2), 107–118 (2005).

[5] Buzzá, H. H., da Silva, A. P., Vollet Filho, J. D., Ramirez, D. P., Trujillo, J. R., Inada, N. M., Moriyama, L. T., Kurachi, C., and Bagnato, V. S., "Photodynamic therapy: progress toward a scientific and clinical network in latin america," *Photodiagnosis and photodynamic therapy* **13**, 261–266 (2016).

Downloaded From: https://www.spiedigitallibrary.org/conference-proceedings-of-spie on 11 Mar 2019
Terms of Use: https://www.spiedigitallibrary.org/terms-of-use

[6] Ramirez, D. P., Kurachi, C., Inada, N. M., Moriyama, L. T., Salvio, A. G., Vollet Filho, J. D., Pires, L., Buzzá, H. H., de Andrade, C. T., Greco, C., et al., "Experience and bcc subtypes as determinants of mal-pdt response: preliminary results of a national brazilian project," *Photodiagnosis and photodynamic therapy* **11**(1), 22–26 (2014).

[7] Soler, A. M., Warloe, T., Berner, A., and Gierckskiy, K. E., "A follow-up study of recurrence and cosmesis in completely responding superficial and nodular basal cell carcinomas treated with methyl 5-aminolaevulinate-based photodynamic therapy alone and with prior curettage," *British Journal of Dermatology* **145**(3), 467–471 (2001).

[8] Calzavara-Pinton, P. G., "Repetitive photodynamic therapy with topical δ-aminolaevulinic acid as an appropriate approach to the routine treatment of superficial non-melanoma skin tumours," *Journal of Photochemistry and Photobiology B: Biology* **29**(1), 53–57 (1995).

[9] Macdonald, I. J. and Dougherty, T. J., "Basic principles of photodynamic therapy," *Journal of Porphyrins and Phthalocyanines* **5**(02), 105–129 (2001).

[10] Dougherty, T. J., Gomer, C. J., Henderson, B. W., Jori, G., Kessel, D., Korbelik, M., Moan, J., and Peng, Q., "Photodynamic therapy," *JNCI: Journal of the National Cancer Institute* **90**(12), 889–905 (1998).

[11] Pogue, B. W., Elliott, J. T., Kanick, S. C., Davis, S. C., Samkoe, K. S., Maytin, E. V., Pereira, S. P., and Hasan, T., "Revisiting photodynamic therapy dosimetry: reductionist & surrogate approaches to facilitate clinical success," *Physics in Medicine & Biology* **61**(7), R57 (2016).

[12] Celli, J. P., Spring, B. Q., Rizvi, I., Evans, C. L., Samkoe, K. S., Verma, S., Pogue, B. W., and Hasan, T., "Imaging and photodynamic therapy: mechanisms, monitoring, and optimization," *Chemical reviews* **110**(5), 2795–2838 (2010).

[13] Kanick, S. C., Davis, S. C., Zhao, Y., Hasan, T., Maytin, E. V., Pogue, B. W., and Chapman, M. S., "Dual-channel red/blue fluorescence dosimetry with broadband reflectance spectroscopic correction measures protoporphyrin ix production during photodynamic therapy of actinic keratosis," *Journal of biomedical optics* **19**(7), 075002–075002 (2014).

[14] Akopov, A. L., Rusanov, A. A., Papayan, G. V., Kazakov, N. V., Gerasin, A. V., and Urtenova, M. A., "Endobronchial photodynamic therapy under fluorescence control: Photodynamic theranostics," *Photodiagnosis and Photodynamic Therapy* **19**, 73–77 (2017).

[15] Sheng, C., Jack Hoopes, P., Hasan, T., and Pogue, B. W., "Photobleaching-based dosimetry predicts deposited dose in ala-ppix pdt of rodent esophagus," *Photochemistry and photobiology* **83**(3), 738–748 (2007).

[16] Zeng, H., Korbelik, M., McLean, D. I., MacAulay, C., and Lui, H., "Monitoring photoproduct formation and photobleaching by fluorescence spectroscopy has the potential to improve pdt dosimetry with a verteporfin-like photosensitizer," *Photochemistry and photobiology* **75**(4), 398–405 (2002).

[17] Boere, I., Robinson, D., De Bruijn, H., Van Den Boogert, J., Tilanus, H., Sterenborg, H. J. C., and de Bruin, R. W. F., "Monitoring in situ dosimetry and protoporphyrin ix fluorescence photobleaching in the normal rat esophagus during 5-aminolevulinic acid photodynamic therapy," *Photochemistry and photobiology* **78**(3), 271–277 (2003).

[18] Mallidi, S., Anbil, S. R., Lee, S., Manstein, D., Elrington, S. A., Kositratna, G., Schoenfeld, D., Pogue, B. W., Davis, S. J., and Hasan, T., "Photosensitizer fluorescence and singlet oxygen luminescence as dosimetric predictors of topical 5-aminolevulinic acid photodynamic therapy induced clinical erythema," *Journal of biomedical optics* **19**(2), 028001 (2014).

[19] Blanco, K. C., Moriyama, L. T., Inada, N. M., Sálvio, A. G., Menezes, P. F., Leite, E. J., Kurachi, C., and Bagnato, V. S., "Fluorescence guided pdt for optimization of the outcome of skin cancer treatment," *Frontiers in Physics* **3**, 30 (2015).

[20] Grecco, C., Buzzá, H. H., Stringasci, M. D., Andrade, C. T., Vollet-Filho, J. D., Pratavieira, S., Zanchin, A. L., Tuboy, A. M., and Bagnato, V. S., "Single led-based device to perform widefield fluorescence imaging and photodynamic therapy," in [*Biophotonics South America*], **9531**, 953121, International Society for Optics and Photonics (2015).

[21] Fujita, A. K. L., Rodrigues, P. G. S., Requena, M. B., Escobar, A., da Rocha, R. W., de Nardi, A. B., Kurachi, C., de Menezes, P. F. C., and Bagnato, V. S., "Fluorescence evaluations for porphyrin formation during topical pdt using ala and methyl-ala mixtures in pig skin models," *Photodiagnosis and photodynamic therapy* **15**, 236–244 (2016).

Downloaded From: https://www.spiedigitallibrary.org/conference-proceedings-of-spie on 11 Mar 2019
Terms of Use: https://www.spiedigitallibrary.org/terms-of-use

[22] Fischer, F., Dickson, E., Pottier, R., and Wieland, H., "An affordable, portable fluorescence imaging device for skin lesion detection using a dual wavelength approach for image contrast enhancement and aminolaevulinic acid-induced protoporphyrin ix. part i. design, spectral and spatial characteristics," *Lasers in medical science* **16**(3), 199–206 (2001).

[23] LaRochelle, E. P., Davis, S. C., de Souza, A. L. R., and Pogue, B. W., "In vivo wide-field multispectral dosimeter for use in ala-ppix based photodynamic therapy of skin," in [*Proc. of SPIE Vol*], **10047**, 1004707–1 (2017).

[24] Roberts, D. W., Olson, J. D., Evans, L. T., Kolste, K. K., Kanick, S. C., Fan, X., Bravo, J. J., Wilson, B. C., Leblond, F., Marois, M., et al., "Red-light excitation of protoporphyrin ix fluorescence for subsurface tumor detection," *Journal of neurosurgery* **128**(6), 1690–1697 (2018).

[25] LaRochelle, E. P., Davis, S. C., de Souza, A. L. R., and Pogue, B. W., "In vivo wide-field multispectral dosimeter for use in ala-ppix based photodynamic therapy of skin," in [*Optical Methods for Tumor Treatment and Detection: Mechanisms and Techniques in Photodynamic Therapy XXVI*], **10047**, 1004707, International Society for Optics and Photonics (2017).

Downloaded From: https://www.spiedigitallibrary.org/conference-proceedings-of-spie on 11 Mar 2019
Terms of Use: https://www.spiedigitallibrary.org/terms-of-use